A DECONVOLVED STRUCTURE OF THE NEBULOSITY ASSOCIATED WITH 3C 206

O. BENDINELLI, G. PARMEGGIANI, and F. ZAVATTI

Dipartimento di Astronomia, Università di Bologna, Italia

(Received 4 February, 1984)

Abstract. The published photographic profile of 3C 206 (reported in the low redshift sample of quasars by Wyckoff *et al.*, 1981) has been deconvolved from the PSF by means of an effective restoration procedure. The deconvolved photometric structure of the quasar consists of a central point-like source, containing 68% of the integrated luminosity, an intermediate region of about 10 kpc radius ($H_0 = 60$ km s^{-1} Mpc^{-1}, $q_0 = 0$) and an external region with nearly-linear slope and brightness level of the profile similar to those of the corresponding regions in giant elliptical and cD galaxies. The result confirms the previous findings in 3C 273, PKS 2135 + 147, and PKS 0812 + 020 obtained in the same way.

1. Introduction

An increasing accuracy of the morphological and spectroscopic work on low redshift quasars ($z \lesssim 0.4$) has revealed that most – if not all – quasars are imbedded in underlying nebulosities with photometric features (see, for instance, Wyckoff *et al.*, 1981, hereafter referred to as WWG; Hutchings *et al.*, 1981; Wlérick *et al.*, 1981; Bothun *et al.*, 1982; Tyson *et al.*, 1982) and spectral continuum (Boroson and Oke, 1982; Boroson *et al.*, 1982; Bergeron *et al.*, 1982; Balick and Heckman, 1983) typical of galaxies at the same distances. All the above mentioned papers bring statistical support to the hypothesis that the quasar phenomenon takes place at the centre of distant galaxies (Sandage, 1971; Kristian, 1973).

A further confirmation of this hypothesis derives from the frequent close association of quasars and faint galaxies with the same redshift (see, e.g., Stockton, 1980, 1982), now observed in several cases. Also it should be noted the presence of weak absorbtion features of stellar origin in some quasars (for instance 3C 48; cf. Boroson and Oke, 1982), and very large H II envelopes in other cases (see, e.g., MR 2251 – 178, Bergeron *et al.*, 1982; and 3C 120, Wlérick *et al.*, 1981). Although from the continuity of spectroscopic and photometric properties between the various types of active nuclei of galaxies and quasars one can expect any morphological type of underlying galaxy, the difficulty of separating the nuclear light from that of the nebulosity has prevented safe interpretation of the optical and spectroscopic features obtained by ground-based observations.

In a previous paper (Bendinelli *et al.*, 1984; hereafter referred to as Paper I) it was shown that the resolved profiles of quasars (i.e., broader than the PSFs (Point-Spread Function), as obtained by deep and large-scale photographic plates) can be deconvolved from the relative PSFs in a rigorous way. By this procedure, there applied to 3C 273,

Astrophysics and Space Science **104** (1984) 199–204. 0004–640X/84/1042–0199$00.90.

PKS 2135 + 147, and PKS 0812 + 020 taken with the PSFs from WWF, the deconvolved profile of the nebulosity underlying 3C 206 is here derived.

2. The Restoration of the Photometric Structure of 3C 206

As in Paper I, a radially-symmetrical model for 3C 206 is assumed 'a priori'. It is composed by a delta-function (the star-like source) at the centre of an underlying nebulosity with smooth brightness profile $\phi(r)$. Further, we assume that an accurate approximation (see Table I) of the normalized stellar profile $f_s(t)$, which defines the

TABLE I

Fit of the PSF of 3C 206

$a_1 = 0.557$	$\sigma_1 = 0.553$
$a_2 = 0.378$	$\sigma_2 = 1.182$
$a_3 = 0.065$	$\sigma_3 = 3.770$

Note: σ_1 in arc sec, mean-square residual 0".06.

Point-spread function (PSF) relative to the quasar observed profile $f_g(r)$, is supplied by a sum of N gaussian functions – i.e.,

$$f_s(r) = \sum_1^N (a_1/2\pi\sigma_1^2) \exp(-r^2/2\sigma_1^2) . \tag{1}$$

Under these assumptions $\phi(r)$ can be derived from the observed profile, sampled at the mesh points x_k ($k = 1, 2, \ldots, M$), by solving the ill-conditioned linear system

$$f_g(x_k) - b \sum_1^N (a_1/2\sigma_1^2) \exp(-x_k^2/2\sigma_1^2) = (1 - b) \sum_1^N \sum_j^M K_1(x_k, x_j)\phi(x_j) . \tag{2}$$

Equation (2) represents the decomposition by means of the parameter b of the observed profile into the light spread by the nucleus (second term at the left-hand side) and the brightness profile of the underlying nebulosity convolved with the PSF (right-hand side term). The problems involved by the solution of Equation (1) and Equation (2) – in particular, numerical stability and uniqueness – are extensively treated in Paper I.

We should emphasize again that a reliable deconvolution of quasar profiles (as shown by numerical experiments in Paper I) requires the PSF to be known over a range of almost 8 mag. or up to the third gaussian component, as obtained in WWG.

Except for the central part, in which the dispersion parameter of the first gaussian, the classical seeing, strictly depends on the site and the time of observations; the agreement of WWG's PSFs with the composite ones obtained by King (1971) and by Capaccioli and de Vaucouleurs (1983) is a confirmation of their reliability. Other

examples of PSFs well defined up to low brightness levels are those given by Strom and Strom (1979) in their study of the surface brightness of galaxies in the cD cluster A401 and by Bothun *et al.* (1982).

Hence, in works dealing with the photometry of extended sources, the behaviour of the PSF can be used as immediate test of accuracy. For instance, an observed profile of 3C 206 rather different from that reported in WWG was obtained by Wyckoff *et al.* (1980), but the sharp downfall of the relative PSF makes it unreliable.

The observed profile of 3C 206 denoted by m_0, its deconvolution m_d and its calculated value m_c are displayed in Figure 1 and reported in Table II. The mean-square residual in the range 0″–4″ and in the whole profile are 0.05 and 0.21 V mag. s^{-2}, respectively. Evidently, most of the discrepancy comes from large fluctuations in the outer observed profile.

The deconvolved structure of 3C 206 from a morphological point of view presents three well-definite components: (1) the central point-like source, containing 68% of the total light, (2) a broad intermediate region, extending up to 10–15 kpc, and (3) an external region, characterized by a quite linear behaviour of the brightness. In Table III, the relevant parameters of the deconvolved structure are compared with the values found in Paper I for the other deconvolved quasars.

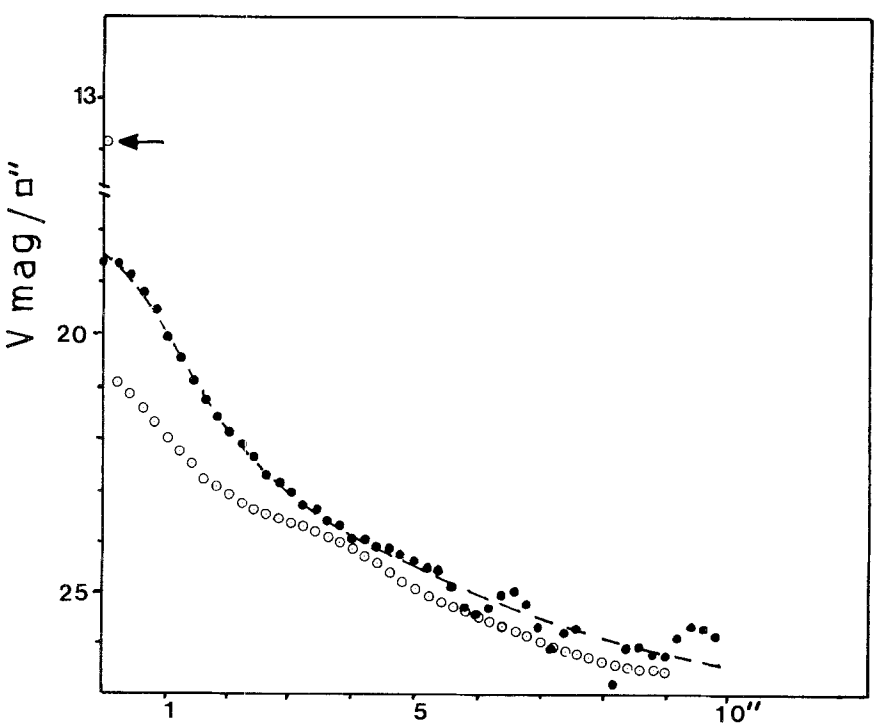

Fig. 1. The WWG observed profile of 3C 206 (dots) and its deconvolution from PSF (circles). The central brightness is indicated by an arrow. The dashed line shows the calculated profile.

TABLE II

The deconvolution of 3C 206

r''	m_0	m_d	m_c	r''	m_0	m_d	m_c
0.0	18.58	13.77	18.66	5.0	24.43	24.92	24.53
0.2	18.68	20.88	18.72	5.2	24.58	25.06	24.64
0.4	18.88	21.11	18.90	5.4	24.63	25.19	24.75
0.6	19.20	21.38	19.19	5.6	24.93	25.30	24.86
0.8	19.55	21.66	19.57	5.8	25.43	25.40	24.97
1.0	20.08	21.95	20.01	6.0	25.43	25.50	25.07
1.2	20.50	22.22	20.48	6.2	25.38	25.60	25.17
1.4	20.88	22.48	20.91	6.4	25.13	25.69	25.27
1.6	21.25	22.80	21.29	6.6	25.08	25.80	25.37
1.8	21.63	22.90	21.61	6.8	25.33	25.90	25.46
2.0	21.90	23.08	21.88	7.0	25.75	26.00	25.56
2.2	22.20	23.23	22.14	7.2	26.08	26.09	25.65
2.4	22.50	23.36	22.39	7.4	25.83	26.18	25.74
2.6	22.75	23.47	22.64	7.6	25.75	26.26	25.83
2.8	22.93	23.57	22.87	7.8	26.00	26.33	25.91
3.0	23.13	23.66	23.09	8.0	26.00	26.40	25.99
3.2	23.30	23.75	23.29	8.2	26.00	26.46	26.06
3.4	23.43	23.85	23.47	8.4	26.13	26.52	26.13
3.6	23.63	23.96	23.63	8.6	26.13	26.56	26.19
3.8	23.75	24.08	23.78	8.8	26.33	26.58	26.25
4.0	24.00	24.20	23.92	9.0	26.33	26.60	26.30
4.2	24.05	24.33	24.05	9.2	25.93	26.61	26.35
4.4	24.13	24.47	24.17	9.4	25.75	26.61	26.39
4.6	24.18	24.62	24.29	9.6	25.83	26.61	26.42
4.8	24.33	24.77	24.41	9.8	25.88	26.61	26.46

TABLE III

Parameters of the photometric structures

	z	b	m_1	m_2	m_3	α^{-1}
PKS 2135 + 147	0.200	0.70	12.33	19.25	21.50	7.85
3C 206	0.200	0.68	13.77	20.88	22.00	6.94
PKS 081 + 020	0.402	0.73	15.50	22.34	23.05	6.38
3C 273	0.158	0.80	9.50	16.03	21.35	16.79

m_1 in V mag. arc sec^{-2}; α^{-1} in kpc ($H_0 = 60$ km s^{-1} Mpc^{-1}, $q_0 = 0$).

By the present method neither the true central brightness nor the spike dimension can be estimated. The mean brightness in the central pixel is m_1, m_2 the central de-spiked brightness (i.e., that of the underlying nebulosity) and finally m_3 and α^{-1} the extrapolated central brightness and the scale factor of the third component, respectively.

3. Discussion

In Paper I, a similarity between the outer brightness profiles of the underlying nebulosities and those in the corresponding regions of the giant elliptical M87 and the cD galaxy NGC 6166 was emphasized.

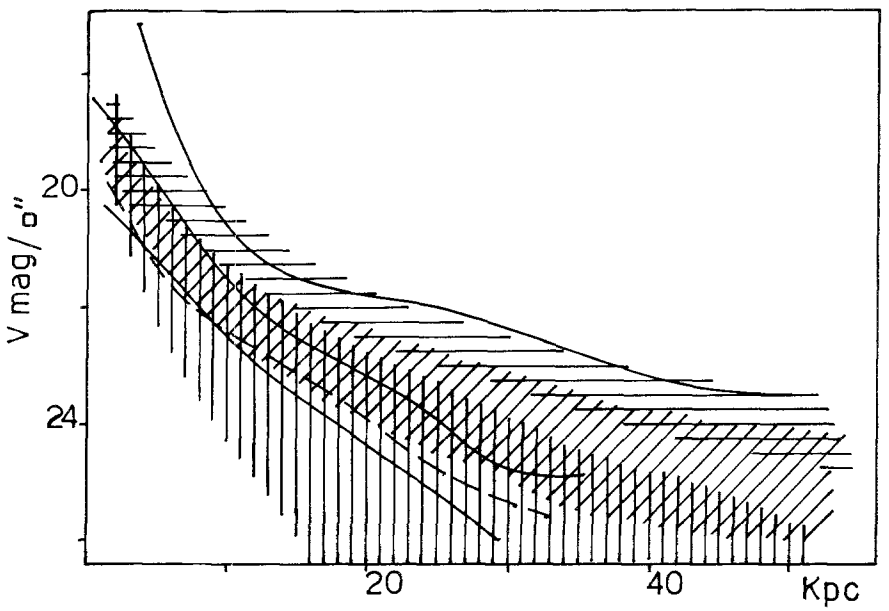

Fig. 2. Comparison of the deconvolved brightness profile of 3C 206 (dashed line) with 3C 273, PKS 2135 + 020, and PKS 0812 + 020 (solid lines, from top to bottom). The upper edge of the X-ray cD galaxies zone (≡) is the brightness profile of A2554 (M_V = 22.61; Valentijn, 1983). The lower edges of the zones defined by cD's in small clusters (// //) and E galaxies in A401 (‖ ‖) are given by MKW 1s (M_v = − 22.61; Thuan and Romanishin, 1981) and D11 (M_v = − 20.22; Strom and Strom, 1979), respectively.

We make here a more extensive comparison (see Figure 2) considering three well-definite samples of galaxies: (1) the X-ray cD galaxies studied by Valentijn (1983), (2) the cD galaxies in poor clusters (Thuan and Romanishin, 1981), and (3) the ellipticals in the cD cluster A401 (Strom and Strom, 1979). Individual galaxies are not shown in Figure 2, but the three groups are indicated as adjacent zones (with small superpositions) in the (m, r)-plane, truncated at the right-hand side before the evident bending of the gEs and cDs profiles according to the modified Hubble law (Oemler, 1976).

One can easily ascertain that, in any subset, there is a great regularity and continuity in shape, so that overlaps are very rare – except near the centres. All the galaxies represented, as well as the quasar underlying nebulosities, were corrected for K-dimming according to Schild and Oke (1971), for galactic absorption (Sandage, 1973), converted to V color and finally corrected for the cosmological dimming factor $(1 + z)^{-4}$.

In Paper I it was shown that the slope of the deconvolved profiles of the nebulosities underlying quasars out to about 10 kpc was similar to the slope observed for gE and cD galaxies in the same radial range. From Figure 2 it appears that the same is true for 3C 206. Also the brightness level of the four quasars today deconvolved by a reliable method is essentially the same of the gEs and cDs in the corresponding region. In the intermediate region of the deconvolved nebulosity (r within ~ 10 kpc), roughly defined by the excess of light respect to the extrapolation towards the centre of the nearly linear

outer profile, the behaviour of 3C 206 confirms the findings of Paper I. There, it was emphasized that the luminosity of this zone seems to increase with the quasar absolute luminosity. Here, it can be argued that it also increases with its whole luminosity. This conflicts with the well-known trend in gEs and cDs, in which the concentration of light near the centre decreases with the absolute luminosity (see Figure 2; or Kron and Albert, 1982).

If the nebulosities underlying quasars are galaxies, the peculiar behaviour of the brightness near the centre may indicate dynamical or chemical evolution due to the quasar presence, and account for the poor evidence of stellar absorption features in spectra taken with the slit some seconds offset from the nucleus.

Finally, it is worth noting that the underlying photometric structures found in the quasars analyzed are in the line of continuity from active nucleus galaxies to quasars. But, as shown in Paper I in the discussion on the appearance of quasar photographic images, the detection of a host normal galaxy (elliptical or spiral), if any, should be searched in very low ($z \lesssim 0.05$) redshift quasars.

References

Balick, B. and Heckman, T. M.: 1983, *Astrophys. J.* **265**, L1.

Bendinelli, O., Parmeggiani, F., Zavatti, F., and Lorenzutta, S.: 1984, *Astrophys. Space Sci.* **103**, 165 (Paper I).

Bergeron, J., Boksenberg, A., Dennefeld, M., and Tarenghi, M.: 1982, *Monthly Notices Roy. Astron. Soc.* (in press).

Boroson, T. A. and Oke, J. B.: 1982, *Nature* **296**, 397.

Boroson, T. A., Oke, J. B., and Green, R. F.: 1982, *Astrophys. J.* **263**, 32.

Bothun, G. O., Romanishin, W., Margon, B., Schommer, R. A., and Chanan, G. A.: 1982, *Astrophys. J.* **257**, 40.

Capaccioli, M. and de Vaucouleurs, G.: 1983, *Astrophys. J. Suppl.* **52**, 465.

Hutchings, J. B., Crampton, D., Campbell, B., and Pritchet, C.: 1981, *Astrophys. J.* **247**, 743.

King, I. R.: 1971, *Publ. Astron. Soc. Pacific* **83**, 199.

Kristian, J.: 1973, *Astrophys. J.* **179**, L129.

Kron, R. G. and Albert, C. E.: 1982, *Publ. Astron. Soc. Pacific* **94**, 887.

Oemler, A.: 1976, *Astrophys. J.* **209**, 693.

Sandage, A. R.: 1971, in D. J. K. O'Connell (ed.), *Pontificiae Academiae Scientiarum Scripta Varia 35, Nuclei of Galaxies*, American Elsevier, New York, p. 271.

Sandage, A. R.: 1973, *Astrophys. J.* **183**, 711.

Schild, R. and Oke, J. B.: 1971, *Astrophys. J.* **169**, 209.

Stockton, A.: 1980, in G. O. Abell and P. J. E. Peebles (eds.), 'Objects of High Red-Shift', *IAU Symp.* **92**, 89.

Stockton, A.: 1982, *Astrophys. J.* **257**, 33.

Strom, S. E. and Strom, K. M.: 1979, *Astron. J.* **84**, 1091.

Thuan, T. X. and Romanishin, W.: 1981, *Astrophys. J.* **248**, 439.

Tyson, J. A., Baum, W. A., and Kreidl, T.: 1982, *Astrophys. J.* **257**, L1.

Valentijn, E. A.: 1983, *Astron. Astrophys.* **118**, 123.

Wlérick, G., Bouchet, P., Cayatte, V., and Michet, D.: 1981, *Astron. Astrophys.* **102**, L17.

Wyckoff, S., Wehinger, P. A., Spinrad, H., and Boksenberg, A.: 1980, *Astrophys. J.* **240**, 25.

Wyckoff, S., Wehinger, P. A., and Gehren, T.: 1981, *Astrophys. J.* **247**, 750 (WWG).